Research Article

Pulmonary Circulation

Right ventricular stroke work correlates with outcomes in pediatric pulmonary arterial hypertension

Weiguang Yang[1], Alison L. Marsden[1,2], Michelle T. Ogawa[1], Charlotte Sakarovitch[1], Keeley K. Hall[1], Marlene Rabinovitch[1] and Jeffrey A. Feinstein[1,2]

[1]Department of Pediatrics (Cardiology), Stanford University, Stanford, CA, USA; [2]Department of Bioengineering, Stanford University, Stanford, CA, USA

Abstract

Pulmonary arterial hypertension (PAH) is characterized by elevated pulmonary artery pressures (PAP) and pulmonary vascular resistance (PVR). Optimizing treatment strategies and timing for transplant remains challenging. Thus, a quantitative measure to predict disease progression would be greatly beneficial in treatment planning. We devised a novel method to assess right ventricular (RV) stroke work (RVSW) as a potential biomarker of the failing heart that correlates with clinical worsening. Pediatric patients with idiopathic PAH or PAH secondary to congenital heart disease who had serial, temporally matched cardiac catheterization and magnetic resonance imaging (MRI) data were included. RV and PA hemodynamics were numerically determined by using a lumped parameter (circuit analogy) model to create pressure-volume (P-V) loops. The model was tuned using optimization techniques to match MRI and catheterization derived RV volumes and pressures for each time point. RVSW was calculated from the corresponding P-V loop and indexed by ejection fraction and body surface area ($RVSW_{EF}$) to compare across patients. Seventeen patients (8 boys; median age = 9.4 years; age range = 4.4–16.3 years) were enrolled. Nine were clinically stable; the others had clinical worsening between the time of their initial matched studies and their most recent follow-up (mean time = 3.9 years; range = 1.1–8.0 years). $RVSW_{EF}$ and the ratio of pulmonary to systemic resistance (Rp:Rs) values were found to have more significant associations with clinical worsening within one, two, and five years following the measurements, when compared with PVR index (PVRI). A receiver operating characteristic analysis showed $RVSW_{EF}$ outperforms PVRI, Rp:Rs and ejection fraction for predicting clinical worsening. $RVSW_{EF}$ correlates with clinical worsening in pediatric PAH, shows promising results towards predicting adverse outcomes, and may serve as an indicator of future clinical worsening.

Keywords

right ventricular failure, clinical worsening, risk stratification, pressure-volume (P-V) loop, lumped parameter model

Date received: 9 September 2017; accepted: 11 May 2018

Pulmonary Circulation 2018; 8(3) 1–9
DOI: 10.1177/2045894018780534

Introduction

Pulmonary arterial hypertension (PAH), defined by a mean pulmonary artery pressure (mPAP) > 25 mmHg with pulmonary capillary wedge pressure < 15 mmHg, leads to structural changes within the pulmonary vasculature, increased right ventricular work, and ultimately cardiac dysfunction. In children, PAH is most commonly either idiopathic (IPAH) or associated with congenital heart disease (PAH-CHD). Disease progression is highly variable and poorly understood. In severe cases, five-year survival rates are poor, approximating only 60–70%.[1,2] As no known cure exists, treatment options are limited to pharmacologic therapies that help to slow disease progression. In the most severe cases, lung or heart–lung transplantation is the only remaining option. As transplantation carries significant morbidity and mortality risks, optimizing PAH treatment strategies and timing of transplant referral and listing remains crucial.[3–5] The development of novel markers of disease

Corresponding author:
Jeffrey A. Feinstein, Department of Pediatrics (Cardiology), Stanford University, 750 Welch Road – Suite 305, Palo Alto, CA 94304, USA.
Email: Jeff.Feinstein@stanford.edu

progression and risk stratification to assist the clinician with transplant referral timing, therefore, is of great importance for this high-risk population.

Currently, the World Health Organization (WHO) functional class (FC) and 6-min walk distance are often used as clinical endpoints for risk-stratification in adult PAH patients. These endpoints, however, are not well characterized in pediatric patients.[6,7] Previous studies have shown that hemodynamic parameters (e.g. cardiac index, pulmonary vascular resistance [PVR], pulmonary to systemic vascular resistance ratio [Rp:Rs], RV function as measured by ejection fraction [EF], and end-diastolic volume index [EDVI]) and circulating biomarkers (e.g. brain natriuretic peptide [BNP]/N-terminal pro-BNP) are valid endpoints that can determine prognosis in pediatric PAH patients.[6,8] However, despite the correlations between these factors and disease severity,[2,6,9] there remains a pressing need for improved predictive markers of clinical worsening.

Pressure-volume (P-V) loops have long been used to characterize ventricular performance, with stroke work defined by the area enclosed within the P-V loop. These measures, however, are most frequently used in the research setting due to the financial and logistical issues associated with routine clinical use. Computational modeling is able to bridge the divide between the research and clinical constraints by extracting hemodynamic quantities that are not routinely measured in clinical practice such as wall shear stress and P-V loops.[10–13] Although P-V loops have been used to assess myocardial contractility and ventricular-arterial coupling for RV pressure overload, right ventricular stroke work (RVSW) has not been calculated from P-V loops for pediatric patients with PAH.[14] Recently, Di Maria et al.[15] showed that RVSW estimated by a simplified formula was associated with WHO FC and adverse outcomes but RVSW was not found be a better predictor as compared to pulmonary vascular resistance index (PVRI). The goal of this study is to quantify RVSW in pediatric PAH patients directly from P-V loops that are produced by computational modeling incorporating routine clinical data and correlate it with clinical outcomes to evaluate RVSW as a potential clinically useful marker of disease severity and clinical worsening.

Methods

Patient selection

Pediatric patients (aged < 18 years) with IPAH or PAH-CHD who underwent right heart catheterization (RHC) and magnetic resonance imaging (MRI) at Lucile Packard Children's Hospital Stanford from July 2006 to August 2015 were eligible for this retrospective study. Serial, matched catheterization and MRI data were collected under an Institutional Review Board approved protocol. The population was further refined to include only individuals who had undergone at least two "paired" RHC/MRI measurements. In order to be "paired," RHC and MRI had to be performed no more than six months apart.

Assessment of right ventricular stroke work

We applied a lumped parameter (circuit analogy) model (Appendix Fig. O1) to simulate RV and PA hemodynamics. Model components included three element Windkessel models of the PAs, a time-varying elastance to model the right ventricle, and a constant pressure to model the right atrium (RA).[13] The tricuspid and pulmonary valves were modeled to account for regurgitation and stenosis.[16] Model parameters were automatically tuned using optimization to match measured clinical values (systolic, diastolic, and mean pressures, flow rates, and end-diastolic and end-systolic volumes [EDV and ESV]) found in catheterization and MRI reports, respectively, for each patient at each time point. The lumped parameter model (LPM) is governed by a set of ordinary differential equations (ODEs), which were solved numerically to produce a P-V loop. Solution of this system can be obtained within 5–10 min on a standard personal computer. The RV stroke work was then determined from the P-V loop by integration (i.e. the area within the P-V loop). Numerical details of the patient specific lumped parameter modeling are provided in the appendix.

For validation purposes, we obtained pressure tracings and time-dependent RV volume curves for two representative patients and created P-V loops directly from the clinical data (cardiac catheterization and MRI, respectively) to compare with those generated by the LPM. The procedure is described as follows. First, RA pressure (RAP), RV pressure (RVP), PAP and ECG signals were extracted from Mac-Lab system (GE Healthcare, Milwaukee, WI, USA) and aligned according to simultaneously recorded ECG signals (R-R interval). Isovolumetric contraction and relaxation are determined by the intersections of RVP-PAP and RVP-RAP curves (Appendix Fig. O2a). Using ECG-gated and breath-held techniques,[17] 20 cardiac phases of multi-slice cine images were recorded yielding a slice thickness of 8 mm and a temporal resolution of 48 ms. Endocardial borders for the RV were segmented by a radiologist on multiple short-axis planes and RV volumes were calculated for each cardiac phase resulting in a time-dependent RV volume curve. EDV and ESV correspond to the smallest and largest points of the RV volume curve. Then the RV volume curve was scaled and aligned with the RVP curve based on the end-systolic point (Appendix Fig. O2a). Although no valvular regurgitation was seen, RV volumes were not constant during isovolumetric contraction and relaxation phases largely due to a relatively low temporal resolution and segmentation errors. Therefore, RV volume curves were corrected by imposing constant ESV and EDV during isovolumetric contraction and relaxation phases. Figure 1 shows a comparison between LPM derived and catheterization-MRI derived P-V loops. The differences in stroke work are within 7% for both patients.

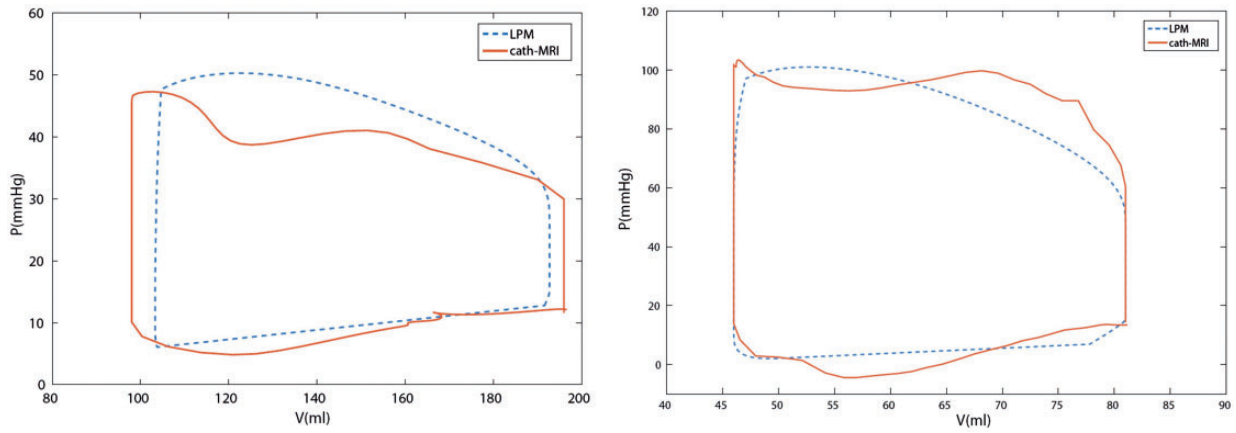

Fig. 1. Comparison of P-V loops derived from LPMs and co-registration of RV pressure signals and volume curves.

To compare RVSW among patients, and over time, RVSW was normalized using an allometric scaling law based on body surface area (BSA). We define $RVSW_{BSA}$ as follows:

$$RVSW_{BSA} = \frac{RVSW}{BSA^{1.407}}$$

$$RVSW = \int_{V(T)}^{V(0)} P(t)dV(t)$$

where P, V, T are RVP (mmHg), RV volume (mL), and cardiac cycle duration(s), respectively. The same allometric scaling law would be appropriate for stroke volume alone, namely $BSA^{1.407}$.[18] At each time point for which both MRI and RHC results were available, a lumped parameter model simulation was performed with matched pressures and volumes, and RVSW was computed. Since RVSW represents the area under the RV P-V loop, two P-V loops with an identical geometry but different EDVs can produce the same RVSW, but obviously represent different "physiologies." In addition, RVSW could be similarly misleading if a second PV-loop featured proportionally reduced stroke volume and increased RVP. To accurately capture differences in the physiology not represented by the area of P-V loops, $RVSW_{BSA}$ is scaled by its corresponding EF,

$$RVSW_{EF} = \frac{RVSW_{BSA}}{EF}$$

Thus, a patient with a low EF can be distinguished from other patients who have similar RVSW by an EF penalized stroke work.

Statistical analysis

We hypothesized that $RVSW_{EF}$ is higher in patients with clinical worsening compared to stable patients. In a patient level analysis, patients were categorized into two groups (stable and clinical worsening) based on the most recent data. Clinical worsening (poor response/poor outcomes) was defined as: (1) death; (2) lung or heart–lung transplant; (3) recommendation and/or active listing for transplant; or (4) hemodynamic worsening despite maximal therapy, specifically intravenous (IV) or subcutaneous (SQ) prostenoids. Patients who were free of all adverse clinical events mentioned above were defined as clinically stable. The Mann–Whitney U test and Fisher's exact test were used to test continuous and categorical data between the two groups.

As patients in this study did not have the same follow-up duration, we analyzed the data at the measurement level, that is taking each MRI/RHC measurement and examining the probability of clinical worsening within one, two, and five years following the measurement. While one, three, and five years are routinely used as endpoints, we chose to use two years instead of three as the waiting time for transplant in outpatients often approximates two years. For each MRI/RHC measurement we defined binary outcomes (stable versus clinical worsening) within one, two, and five years. Measurements after August 2016 were not included as follow-up was not long enough to define clinical stability. For each MRI/RHC measurement, we analyzed $RVSW_{EF}$, PVRI, and Rp:Rs. Associations between each marker and each outcome were tested with a mixed model designed to account for correlations among measurements from the same patient. P values ≤ 0.05 were considered statistically significant and no adjustment on multiple testing was performed. Pearson's linear correlation coefficients were computed to examine correlations between predictors. An R package, survivalROC, was used to perform a time-dependent receiver operating characteristic (ROC) analysis (cumulative sensitivity and dynamic specificity, C/D) to identify cut-off values for predictors.[19,20] The most recent predictor values at time t since diagnosis were used to create ROC curves for predicting clinical worsening at time $t+\Delta t$. We chose $t=2$ and 4 years since diagnosis and $\Delta t=$ 2 and 5 years. A control was defined as any patient remaining stable without clinical worsening at time $t+\Delta t$

and a case is defined as any patient presenting clinical worsening between t and t+Δt. Note that a control may become a case if Δt is increased.

Results

Patient recruitment and description

We identified 17 patients (8 boys; average age = 9.4 years; age range = 4.4–16.3 years) in the study, 12 with IPAH and the remaining 5 with PAH-CHD. Nine patients remained clinically stable at the most recent follow-up, while the remaining 8 patients had clinical worsening: death (n = 2); heart–lung transplant indicated (n = 2) or performed (n = 3); and poor hemodynamic response to IV prostanoids (n = 1). All patients classified in the clinical worsening group were found to remain in that group for the duration of the study period. Patient characteristics from the initial MRI/RHC measurements are summarized overall and by clinical outcome groups in Table 1. A total of 61 MRI/RHC "pairs" were collected for the 17 patients. The median time difference between paired RHC and MRI is 1 day (range = 0–153 days). Seven pairs were matched with 3–5 months (time between studies). Average time between diagnosis and first MRI/RHC pair was 2.9 ± 2.3 and 1.5 ± 1.3 years, for the stable and worsening groups, respectively. The median (interquartile range [IQR]) follow-up time between first and most recent pairs was 4.2 (3.1–5.2) and 3.7 (1.9–4.9) years for the stable and worsening groups, respectively.

Right ventricular stroke work

P-V loops generally become larger and rightwards over time, with increasing RVSW, in patients with clinical worsening, as shown for two representative patients in Fig. 2. $RVSW_{EF}$ values for clinically stable patients (as determined at the most recent time point for each) generally trended downward and/or remained lower over time compared to those who progressed to clinical worsening (Fig. 3).

The distribution of the three quantities of interest ($RVSW_{EF}$, PVRI, and Rp:Rs values) according to our three outcomes (clinical worsening at one, two, and five years) are represented in Fig. 4. The one-year clinical outcome was available for each of the 61 measurements while one was missing for the two-year outcome and the five-year outcome was available only for 50 measurements. $RVSW_{EF}$ and Rp:Rs were significantly elevated for patients with clinical worsening within one, two, and five years compared to

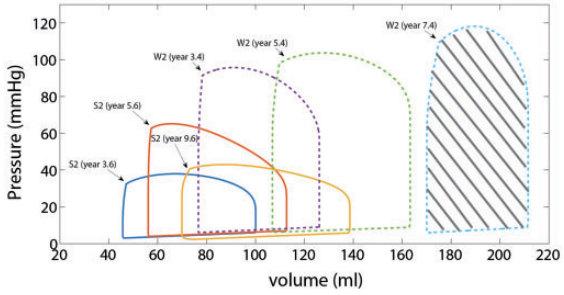

Fig. 2. P-V loop examples. P-V loops shown for two patients, one clinically stable (S2) and one with clinical worsening (W2) over time. P-V loops are generated by a lumped parameter model described in Appendix to match catheterization measured RVP and PAP and MRI-derived RV volumes. RVSW is calculated as the area under the curve (e.g. shaded area for patient W2 [year 7.4]). P-V loops for patients who clinically worsened generally tended to be larger and rightward.

Table 1. Characteristics of PAH patients at first RHC/MRI measurement.

	All patients (n = 17)	Stable (n = 9)	Worsening (n = 8)	*P* value
Male (n (%))	8 (47)	4 (44)	4 (50)	0.36
Age (years)	8.6 (4.3–16.3)	10.7 (4.9–16.3)	8.4 (4.4–13.5)	0.48
Follow-up period (years)	4.2 (1.1–8)	4.2 (1.2–8)	3.7 (1.1–6)	0.3
Time between diagnosis and first RHC/MRI measurement (years)	1.8 (0–7)	3.4 (0–7)	1.6 (0–3.4)	0.13
Prostacyclin therapy (n)	10	3	7	0.03
BSA (m^2)	0.95 (0.6–1.8)	1.0 (0.6–1.7)	0.9 (0.7–1.8)	0.96
IPAH (n)	12	5	7	0.16
PVRI (WU×m^2)	10.7 (5.2–31.6)	6.8 (5.2–31.6)	14.8 (8.1–24.7)	0.01
RVEF (%)	48 (18–55)	48 (30–55)	48 (18–54)	0.76
RVEDVI (mL/m^2)	105 (81–303)	90 (81–132)	108 (93–303)	0.16
LVSVI (mL/m^2)	45 (23–53)	45 (30–53)	42 (23–52)	0.56
LVEDVI (mL/m^2)	68 (50–97)	67 (57–97)	71 (50–81)	0.74

Data are shown as the median (minimum–maximum).

RHC, right heart catheterization; MRI, magnetic resonance imaging; BSA, body surface area; IPAH, idiopathic pulmonary arterial hypertension; PVRI, pulmonary vascular resistance index; RVEF, right ventricular ejection fraction; RVEDVI, right ventricular end diastolic volume index; LVSVI, left ventricular stroke volume index; LVEDVI, left ventricular end diastolic volume index.

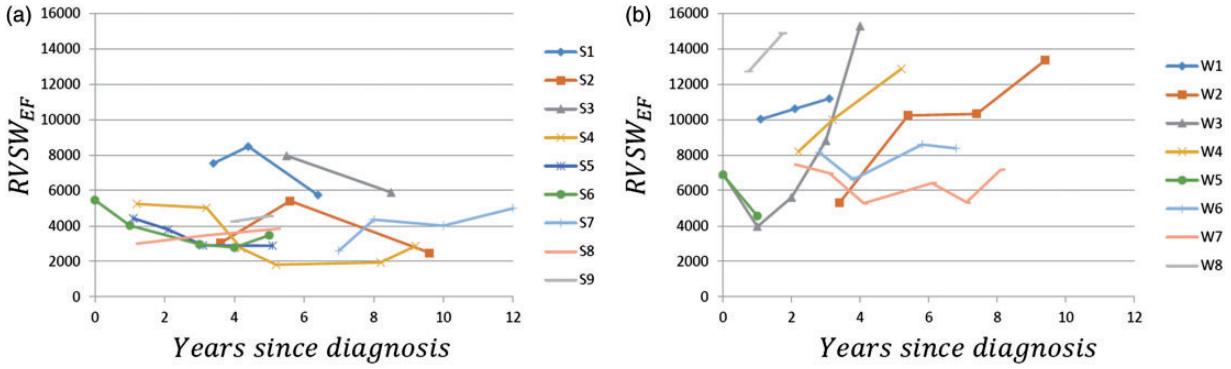

Fig. 3. Longitudinal $RVSW_{EF}$ by group (stable (a) vs. clinical worsening (b)). An upward trend in $RVSW_{EF}$ over time is observed for patients who demonstrated clinical worsening, while the trend for stable patients is downward.

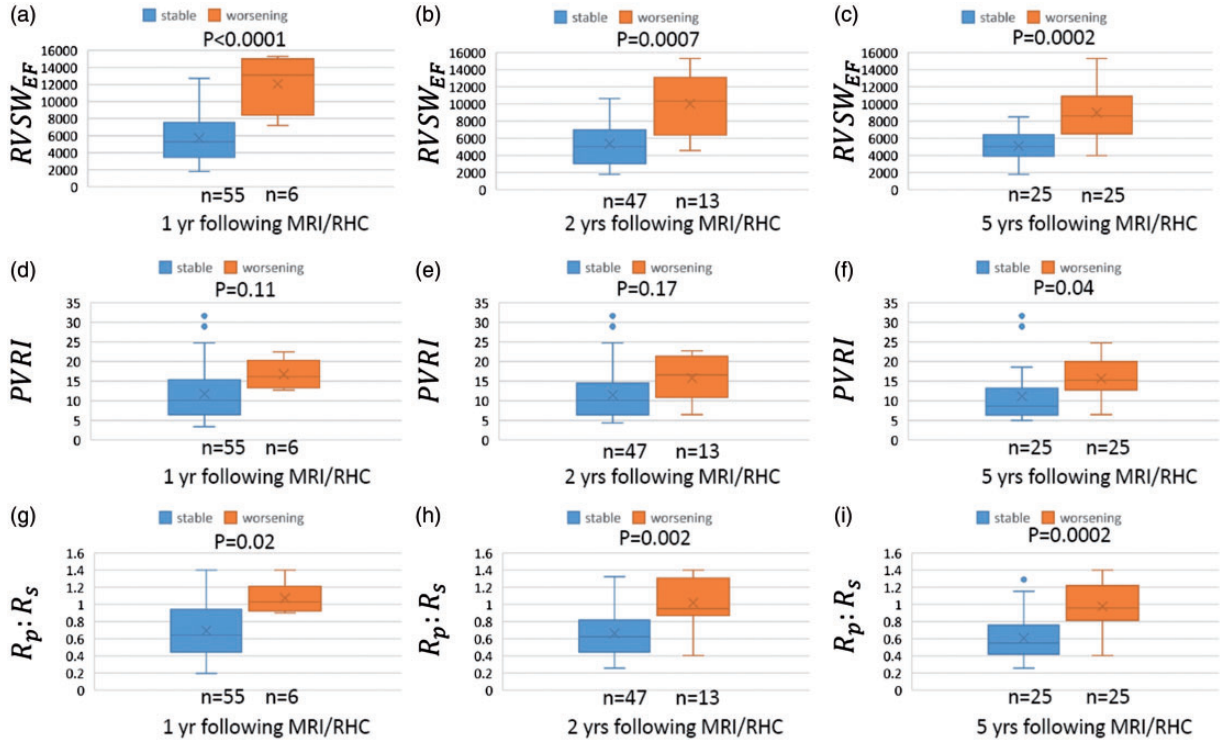

Fig. 4. Comparison of $RVSW_{EF}$, PVRI, and Rp:Rs with stable and worsening outcomes. For each MRI/RHC measurement, $RVSW_{EF}$, PVRI, and Rp:Rs are grouped by the outcomes (stable or worsening) within 1, 2, and 5 years after the measurement and represented by box-whisker plots. The first and third quartiles are at the ends of the box. The median and mean values are indicated by a line and a cross sign. The maximum and minimum are at the ends of the whiskers. Outliers (>1.5 times IQR) are represented by dots.

those in clinically stable patients ($P < 0.0001$, $P = 0.0007$, and $P = 0.0002$ for $RVSW_{EF}$; $P = 0.02$, $P = 0.002$, and $P = 0.0002$ for Rp:Rs; Fig. 4). In contrast, PVRI does not correlate with one- and two-year clinical status ($P = 0.11$ and $P = 0.1$, respectively). Visually, both $RVSW_{EF}$ and Rp:Rs have a relatively smaller overlapping range between the two groups compared to PVRI at all time points in Fig. 4. In addition, the $RVSW_{EF}$ data points are more clustered than the PVRI and Rp:Rs data points, which both contain outliers, defined as > 1.5 times the IQR (Fig. 4d–f, i).

The correlations between $RVSW_{EF}$ and PVRI was found to be moderate and statistically significant ($r^2 = 0.38$, $P < 0.0001$; Fig. 5). These tended to correlate more closely with lower PVRI values and less well for higher PVRI. $RVSW_{EF}$ was weakly correlated with pro-BNP ($r^2 = 0.16$, $P = -0.01$).

We found 10 and 13 patients available for time-dependent ROC analysis in years 2 and 4, respectively. Overall, $RVSW_{EF}$, Rp:Rs, and EDVI outperformed PVRI and EF for two- and five-year predictions. Table 2 shows the area

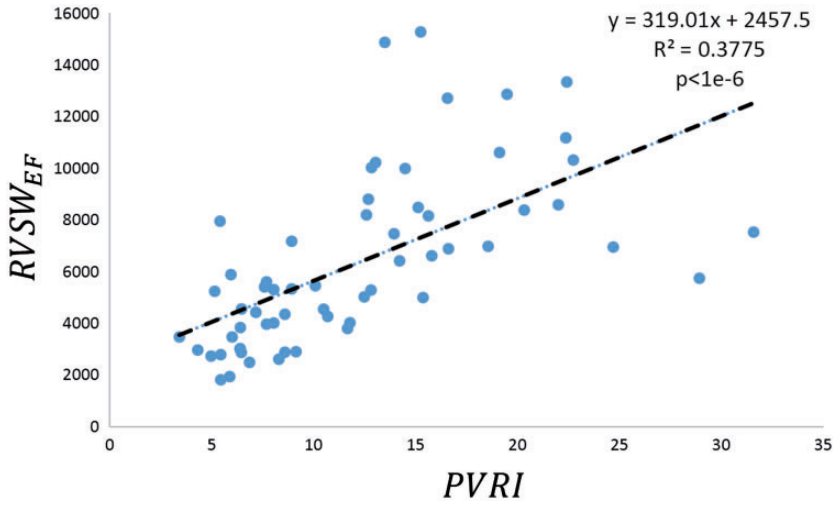

Fig. 5. Correlations between $RVSW_{EF}$ and PVRI. $RVSW_{EF}$ correlates better with PVRI when $RVSW_{EF} < 10{,}000$ and $PVRI < 20$.

Table 2. ROC performance of $RVSW_{EF}$, PVRI, Rp:Rs, EF, and RVEDVI.

	$\Delta t = 2$ years				$\Delta t = 5$ years			
	AUC	Cut-off	Spec.	Sen.	AUC	Cut-off	Spec.	Sen.
t = year 2								
$RVSW_{EF}$	0.70	8191.9	0.90	0.46	0.83	7466.2	0.90	0.55
PVRI	0.41	13.5	0.75	0.07	0.69	13.5	0.91	0.33
Rp:Rs	0.62	0.83	0.80	0.19	0.89	0.72	0.87	0.69
EF	0.01	39%	0	0.25	0.09	48%	0.25	0.09
RVEDVI	0.72	121	0.90	0.39	0.81	104.7	0.90	0.70
t = year 4								
$RVSW_{EF}$	0.98	6615.3	0.92	1.0	0.90	6615.3	0.89	0.52
PVRI	0.89	15.3	0.94	0.44	0.79	15.1	0.90	0.35
Rp:Rs	0.96	0.8	0.93	0.93	0.78	1.03	0.93	0.20
EF	0.20	41%	0.29	0.15	0.44	49%	0.61	0.22
RVEDVI	0.98	105.0	0.92	0.87	0.62	108.0	0.91	0.32

AUC, area under curve; Sen., sensitivity; Spec., specificity.

under the curve (AUC), cut-off values with sensitivity and specificity in four conditions. For predicting two-year outcomes, we observed a large improvement in AUC from year 2 to year 4 for all predictors. It is likely because a small case number (n = 3) for predicting two-year outcomes made AUC sensitive to the variations in cases. Rather than choose a cut-off value with equal weight given to sensitivity and specificity, given the significant mortality associated with lung transplant, a high sensitivity was chosen to prevent "early transplantation listing". For a specificity of about 0.9, optimal cut-off $RVSW_{EF}$ was found between 6615 and 8192 $mmHg \times mL/(m^2)^{1.407}$ with a sensitivity in the range of 0.46–1 when the time at measurement and prediction time were varied. Performance for Rp:Rs and RVEDVI was optimal for predicting five-year outcomes in year 2 but was less consistent than that for $RVSW_{EF}$.

Discussion

This study proposes a computational modeling-based RVSW as a novel, potential biomarker and predictor of clinical worsening in pediatric PAH patients. We collected longitudinal RHC and MRI data for pediatric patients with PAH, and calculated RVSW using a lumped parameter model tuned to match in vivo measurements.

An upward trend in $RVSW_{EF}$ over time is observed for patients who demonstrated clinical worsening, while the trend for stable patients is downward (Fig. 3). While most patients' results followed the general trends, a few outlier cases can be observed in Fig. 3. Unlike the overall trend for the group with clinical worsening, $RVSW_{EF}$ for patient W5 decreased with time. This particular patient was a five-year-old girl with systemic juvenile idiopathic arthritis (SJIA).

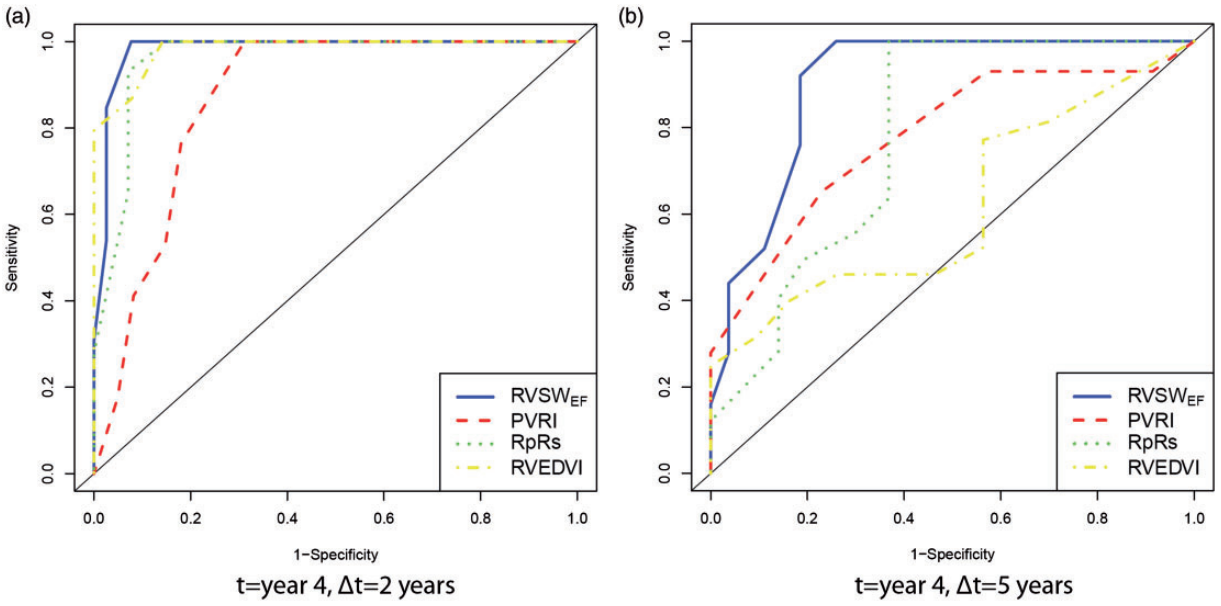

Fig. 6. Time-dependent ROC curves for predicting clinical worsening (a) 2 and (b) 5 years after year 4 since diagnosis using $RVSW_{EF}$, PVRI, Rp:Rs, and RVEDVI.

Her degree of pulmonary hypertension (PH) correlated well with the control (or lack thereof) of her JIA. The initial RVSW point was during a mild JIA flare, while the second, and lower, point represented a time of excellent clinical health after pharmacologic intervention for her PAH. She subsequently experienced a severe JIA flare, with severe PH and died after a four-week stay in the intensive care unit. Had RVSW parameters been obtained during that hospitalization, they most certainly would have demonstrated a significantly elevated RVSW as, by echo, her PAPs were significantly higher, her RV size larger, and ejection fraction smaller. Given her initial $RVSW_{EF}$ was greater than that of most stable patients, one could argue that a high level of concern would be appropriate despite the improvement over time. Patient W3 is a 12-year-old with IPAH who presented with severe disease as evidenced by syncope. The initial decrease in $RVSW_{EF}$ accompanies her initial response to epoprostenol, while the subsequent steep ascent correlates with her subsequent clinical course and the well described clinical worsening over time of many pediatric patients on this therapy.[21,22]

To control the influence of variable length of follow-up among the patients, for each data point, outcomes were compared at one, two, and five years following each MRI/RHC measurement. We showed that $RVSW_{EF}$ is significantly elevated for the clinical worsening group at one, two, and five years when compared with the stable group. Similarly Rp:Rs, a metric currently routinely used in clinical practice, was also significantly different between stable and worsening groups. For PVRI, elevated outliers in the stable group and a higher degree of overlap between two groups makes it a less reliable predictor compared to $RVSW_{EF}$ and Rp:Rs. This overlap was likely due to high longitudinal variability. In contrast, we observed relatively consistent increases for $RVSW_{EF}$ among patients with clinical worsening.

Time-dependent ROC analysis was performed to identify cut-off values and compare the performance of these predictors. Overall, $RVSW_{EF}$, Rp:Rs, and RVEDVI outperform PVRI and EF with a larger AUC. The superiority of $RVSW_{EF}$ over Rp:Rs and EDVI was not clear in time-dependent ROC analysis likely due to a small sample size. ROC results are consistent with our direct observation in Fig. 3 that $RVSW_{EF}$ for patients without clinical worsening trended to or remained < 6000 while the clinical worsening group showed worsening $RVSW_{EF}$ and/or values consistently > 6000–8000. Patients S1 and S3's $RVSW_{EF}$ values were elevated approaching 8000 at the first MRI/RHC measurements but were brought down successfully in the following management.

Generally, RVSW increases with increasing PVRI. Since RVSW is a product of pressure and volume and the RV stroke volume is not linearly correlated with PVR, the strength of the linear relationship between $RVSW_{EF}$ and PVRI is greatly reduced. Similarly, NT-proBNP did not correlate with $RVSW_{EF}$.

Di Maria et al.[15] estimated RVSW in children with PAH by multiplying mPAP by stroke volume. Although a simplified formula was employed and only 1 data point was collected for each patient, RVSW was still found to be correlated with WHO FC and adverse outcomes.[15] However, estimated RVSW for patients with death, septostomy, or WHO FC IV did not significantly differ from that for patients with WHO FC $\leq$ III.[15] This was likely caused by decreased RVSW in patients with WHO FC IV, which is consistent with our non-normalized longitudinal results.

As illustrated in Fig. 2, the first two P-V loops for patient W2 show increased RVSW (area under the P-V loop) whereas the third P-V loop (shaded) becomes slender with reduced RVSW and EF (20%). Thus, using a single RVSW point or monitoring RVSW only without normalizing against EF or considering additional metrics, may misclassify an advanced stage as a hemodynamically improved condition. RVSW was not found to be superior to PVRI as a prognostic predictor.[15] In contrast, we used an EF penalized index, $RVSW_{EF}$, to ameliorate this drawback of RVSW and demonstrated that $RVSW_{EF}$ better predicts clinical worsening than PVRI and Rp:Rs. For our cohort of patients, the simplified formula proposed by Di Maria et al. underestimates RVSW by up to 35% compared to our computational modeling derived RVSW. Chemla et al.[24] compared several formulas for estimating RVSW and also found the classic formula markedly underestimates RVSW.

A major advantage of our method is the generation of patient-specific P-V loops within a standard clinical workflow, since the LPM takes routinely measured single values as inputs. We showed that LPM derived P-V loops agree well with those generated by processing pressure tracings and cine images, which are not routinely reported and can be time-consuming to obtain. Otherwise, expensive P-V catheters or MRI-guided catheterization[14] are required to directly (and invasively) measure P-V loops. Comparisons against directly measured in vivo P-V loop measurements are warranted in future studies to further validate the accuracy of our LPM as well as other simplified formulas for RVSW.

Limitations

Due to unequal numbers of matched studies and duration of follow-up, some patients classified as clinically stable may have been misclassified due to short follow-up. Therefore, values and changes in RVSW and PVRI over time between patients with and without clinical worsening were not directly compared. Instead, outcomes following each MRI/RHC measurement were examined, allowing us to make unbiased classifications and comparisons. Thus, the number of worsening and stable cases is not even for the one- and two-year outcomes.

To enable the collection of a reasonably large dataset given the relatively small patient population, the maximal allowable time between RHC and MRI for the studies to be matched was defined as six months. While results were strong despite this limitation, future studies should attempt to shorten the time between studies to further optimize predictive RVSW parameters. Alternatively, multiple RVSW risk scores could be generated for variable temporal relationships (i.e. MRI/RHC within six months, three months, etc.).

Due to a small sample size, we had to use fewer data points for time-dependent ROC analysis. Sparse data and uneven follow-up may affect statistical results. The cut-off values may or may not represent a number applicable to the more global PH population. Further studies with a greater number of patients would be necessary to further refine the most appropriate cut-off value and compare the performance between predictors.

Conclusion

This study reveals significant associations between outcomes and RVSW in pediatric PAH patients, introducing $RVSW_{EF}$ as a novel metric for clinical worsening. Previously, clinical determination of P-V loops had been limited to research protocols, as their acquisition requires specialized catheters. Our method now has the potential to make P-V loops and RVSW routinely available for clinical use through an efficient lumped parameter model, automatically tuned to match standard RHC and MRI measurements. This will enable clinical quantification of RVSW, which may aid in clinical decision-making to improve treatment and transplant referral algorithms.

Acknowledgments

This work was funded in part by the Vera Moulton Wall Center at Stanford University, and NSF CAREER award OCI 1150184. The authors thank Drs. Aya Kino, Kathrin Baeumler, Jian Wang, Kang Wang, and Jin Long and Prof. Lu Tian for their helpful suggestions and expertise in medical imaging and statistics.

Conflict of interest

The author(s) declare that there is no conflict of interest.

ORCID iD

Weiguang Yang http://orcid.org/0000-0003-3324-4346

References

1. Van Loon RLE, Roofthooft MTR, Delhaas T, et al. Outcome of pediatric patients with pulmonary arterial hypertension in the era of new medical therapies. *Am J Cardiol* 2010; 106(1): 117–124.
2. Beghetti M and Berger RMF. The challenges in paediatric pulmonary arterial hypertension. *Eur Respir Rev* 2014; 23(134): 498–504.
3. Feinstein JA. Evaluation, risk stratification, and management of pulmonary hypertension in patients with congenital heart disease. Semin Thorac Cardiovasc Surg *Pediatr Card Surg Annu* 2009; 106–111.
4. Lordan JL and Corris PA. Pulmonary arterial hypertension and lung transplantation. *Expert Rev Respir Med* 2011; 5(3): 441–454.
5. Goldstein BS, Sweet SC, Mao J, et al. Lung transplantation in children with idiopathic pulmonary arterial hypertension: an 18-year experience. *J Heart Lung Transplant* 2011; 30(10): 1148–1152.
6. Takatsuki S and Ivy DD. Current challenges in pediatric pulmonary hypertension. *Semin Respir Crit Care Med* 2013; 34(5): 627–644.

7. Rosenzweig EB, Feinstein JA, Humpl T, et al. Pulmonary arterial hypertension in children: Diagnostic work-up and challenges. *Prog Pediatr Cardiol* 2009; 27(1): 4–11.
8. Moledina S, Pandya B, Bartsota M, et al. Prognostic significance of cardiac magnetic resonance imaging in children with pulmonary hypertension. *Circ Cardiovasc Imaging* 2013; 6(3): 407–414.
9. Hopper RK, Abman SH and Ivy DD. Persistent challenges in pediatric pulmonary hypertension. *Chest* 2016; 150(1): 226–236.
10. Tang BT, Fonte TA, Chan FP, et al. Three-dimensional hemodynamics in the human pulmonary arteries under resting and exercise conditions. *Ann Biomed Eng* 2011; 39(1): 347–358.
11. Tang BT, Pickard SS, Chan FP, et al. Wall shear stress is decreased in the pulmonary arteries of patients with pulmonary arterial hypertension: An image-based, computational fluid dynamics study. *Pulm Circ* 2012; 2(4): 470–476.
12. Marsden AL and Esmaily-Moghadam M. Multiscale modeling of cardiovascular flows for clinical decision support. *Appl Mech Rev* 2015; 67(3): 030804.
13. Migliavacca F, Pennati G, Dubini G, et al. Modeling of the Norwood circulation: effects of shunt size, vascular resistances, and heart rate. *Am J Physiol Heart Circ Physiol* 2001; 280(5): H2076–2086.
14. Kuehne T, Yilmaz S, Steendijk P, et al. Magnetic resonance imaging analysis of right ventricular pressure-volume loops: in vivo validation and clinical application in patients with pulmonary hypertension. *Circulation* 2004; 110(14): 2010–2016.
15. Di Maria MV, Younoszai AK, Mertens L, et al. RV stroke work in children with pulmonary arterial hypertension: estimation based on invasive haemodynamic assessment and correlation with outcomes. *Heart Br Card Soc* 2014; 100(17): 1342–1347.
16. Mynard JP, Davidson MR, Penny DJ, et al. A simple, versatile valve model for use in lumped parameter and one-dimensional cardiovascular models. *Int J Numer Methods Biomed Eng* 2012; 28(6–7): 626–641.
17. Blalock S, Chan F, Rosenthal D, et al. Magnetic resonance imaging of the right ventricle in pediatric pulmonary arterial hypertension. *Pulm Circ* 2013; 3(2): 350–355.
18. Buechel EV, Kaiser T, Jackson C, et al. Normal right- and left ventricular volumes and myocardial mass in children measured by steady state free precession cardiovascular magnetic resonance. *J Cardiovasc Magn Reson* 2009; 11: 19.
19. Heagerty PJ, Lumley T and Pepe MS. Time-dependent ROC curves for censored survival data and a diagnostic marker. *Biometrics* 2000; 56(2): 337–344.
20. Kamarudin AN, Cox T and Kolamunnage-Dona R. Time-dependent ROC curve analysis in medical research: current methods and applications. *BMC Med Res Methodol* 2017; 17(1): 53.
21. Siehr SL, Ivy DD, Miller-Reed K, et al. Children with pulmonary arterial hypertension and prostanoid therapy: long-term hemodynamics. *J Heart Lung Transplant* 2013; 32(5): 546–552.
22. Siehr SL, Feinstein JA, Yang W, et al. Hemodynamic effects of phenylephrine, vasopressin, and epinephrine in children with pulmonary hypertension: a pilot study. *Pediatr Crit Care Med* 2016; 17(5): 428–437.
23. Ivy DD, Rosenzweig EB, Lemarié J-C, et al. Long-term outcomes in children with pulmonary arterial hypertension treated with bosentan in real-world clinical settings. *Am J Cardiol* 2010; 106(9): 1332–1338.
24. Chemla D, Castelain V, Zhu K, et al. Estimating right ventricular stroke work and the pulsatile work fraction in pulmonary hypertension. *Chest* 2013; 143(5): 1343–1350.